GS2019-2

Preliminary results of bedrock mapping in the Gemmell Lake area, Lynn Lake greenstone belt, northwestern Manitoba (parts of NTS 64C11, 14)

by X.M. Yang

In Brief:
- Detailed bedrock mapping provides an updated geological framework for gold mineralization
- Gold mineralization is hosted in mylonite and silicified-sericitized felsic volcanic to volcaniclastic rocks and in quartz diorite intrusions
- Quartz diorite intrusions of the Post-Sickle intrusive suite may provide an important guide to gold mineralization

Citation:
Yang, X.M. 2019: Preliminary results of bedrock mapping in the Gemmell Lake area, Lynn Lake greenstone belt, northwestern Manitoba (parts of NTS 64C11, 14); *in* Report of Activities 2019, Manitoba Agriculture and Resource Development, Manitoba Geological Survey, p. 10–29.

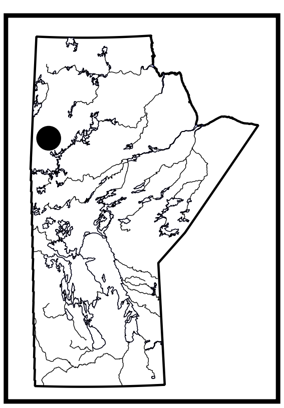

Summary

In 2019, the Manitoba Geological Survey continued a multiyear bedrock mapping project in the Paleoproterozoic Lynn Lake greenstone belt. Detailed mapping at 1:20 000 scale was focused on the southern supracrustal belt in the Gemmell Lake area to resolve some of the key questions about the relationship of Au mineralization to structures, hostrocks, granitoid intrusions and tectonic evolution, and to support ongoing exploration activity in the belt. Preliminary mapping indicates that the area is underlain dominantly by the Wasekwan group supracrustal rocks, comprising massive to pillowed basalt, basaltic andesite, dacite to rhyolite and related volcaniclastic rocks, and subordinate sedimentary rocks. The volcanic sequence is spatially and temporally associated with reworked volcaniclastic and epiclastic rocks, suggestive of deposition in a setting comparable to modern volcanic arcs or back-arc basins. Unconformably overlying the Wasekwan group are the Sickle group sandstone and polymictic conglomerate, which are interpreted to have formed in localized synorogenic basin(s). A set of intrusions divided into pre-Sickle, post-Sickle and late intrusive suites cuts the supracrustal rocks, which were subjected to multiple phases (D_1 to D_6) of deformation and metamorphism.

Two styles of Au mineralization are evident in the map area: 1) Au-bearing mylonite and silicified-sericitized (±disseminated arsenopyrite, pyrite) felsic volcanic to volcaniclastic rocks controlled by the Johnson shear zone, which is related to D_2 deformation and intersected by D_3 faults and associated structures; and 2) intrusion-hosted Au-bearing quartz (±carbonate, sulphide) vein systems controlled by intersections of D_4 faults and the D_2 Johnson shear zone. Although the source of auriferous fluids is enigmatic, the field relationships suggest that timing of the Au mineralization was syn- to post-D_2 deformation. The D_2 event postdated the pre-Sickle intrusions, postdated or was contemporaneous with the post-Sickle intrusive suites, and predated the late intrusive suite. The post-Sickle adakite-like quartz diorite intrusions (subunit 7a) were likely emplaced in a post-subduction extensional setting resulting from the upwelling of asthenosphere mantle due to the rollback of the subducting slab (or collapse of the orogen and/or relaxation due to delamination from the base of thickened lithosphere after terminal terrane collision). This was accompanied by anomalous heating that may have triggered the upward migration of auriferous fluids from the lower crust or upper lithosphere mantle along deep fault(s) connecting to the Johnson shear zone and associated structures in the middle to upper crust, consequently concentrating Au mineralization in favourable sites (e.g., chemical-structural traps). Simultaneously, these processes led to the formation of restricted synorogenic basin(s) that were filled by the Sickle group sediments, eroded from the uplifted greenstone belt.

Introduction

Detailed mapping at 1:20 000 scale in the summer of 2019 was concentrated on the Gemmell Lake area in the southern belt of the Lynn Lake greenstone belt (LLGB; Figure GS2019-2-1), where Au mineralization displays features distinct from those at the MacLellan, Gordon (formerly Farley Lake) and Burnt Timber Au deposits elsewhere in the LLGB. Gold mineralization in the mapping area occurs either as 1) Au-bearing silicified-sericitized mylonite and sheared felsic volcanic to volcaniclastic rocks (±very fine grained arsenopyrite, pyrite disseminations) confined by the Johnson shear zone (JSZ), which is intersected by north-northwest-trending fault structures (e.g., the Gemmell Lake Au

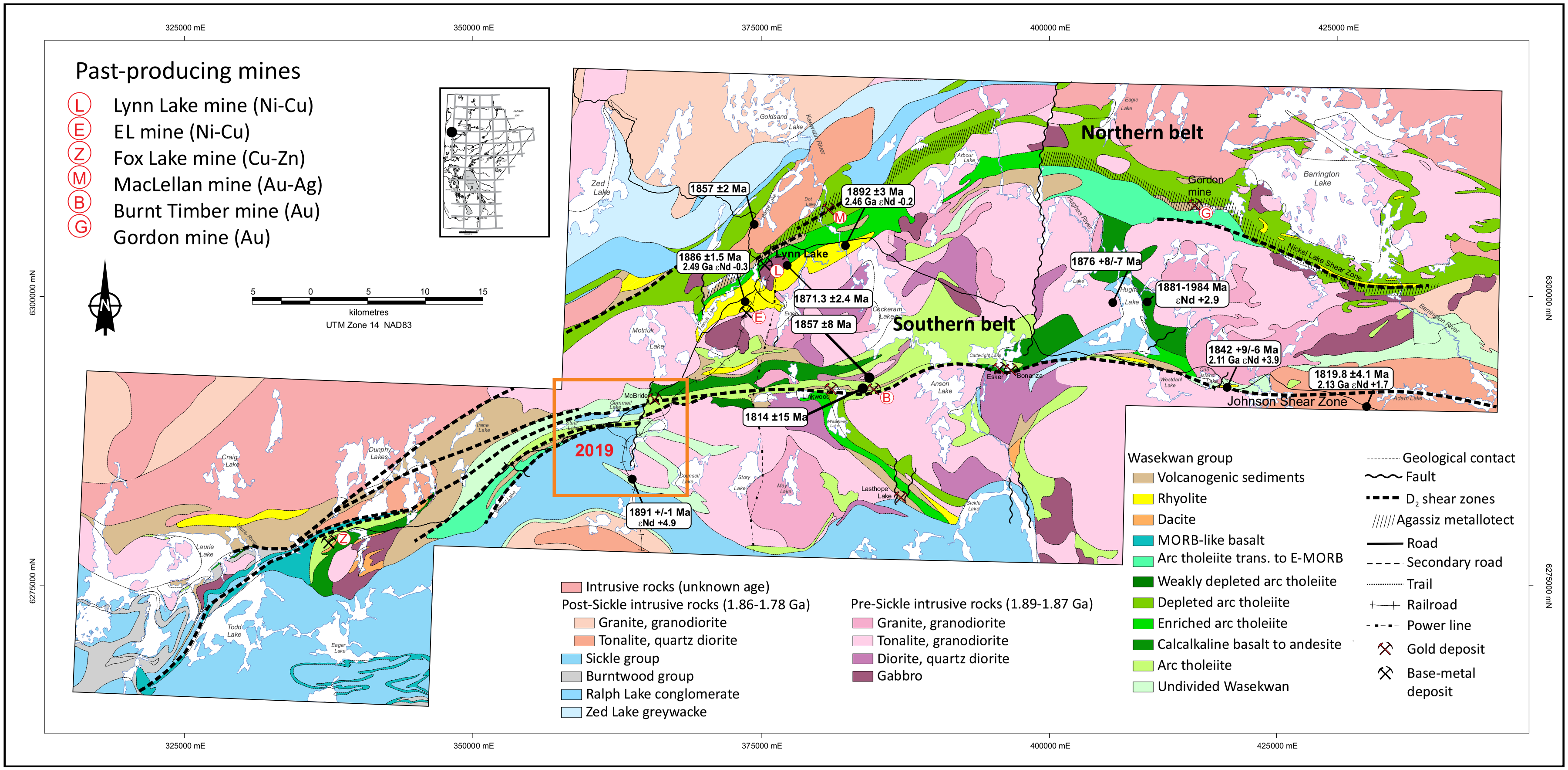

Figure GS2019-2-1: *Regional geology with U-Pb zircon ages and Nd isotopic compositions of the Lynn Lake greenstone belt (modified and compiled from Gilbert et al., 1980; Manitoba Energy and Mines, 1986; Gilbert, 1993; Zwanzig et al., 1999; Turek et al., 2000; Beaumont-Smith and Böhm, 2002, 2003, 2004; Jones, 2005; Beaumont-Smith et al., 2006; Jones et al., 2006; Beaumont-Smith, 2008; Yang and Beaumont-Smith, 2015b, 2016, 2017). The 2019 mapping area is indicated by the orange box. Abbreviation: E-MORB, enriched mid-ocean–ridge basalt.*

occurrence; Beaumont-Smith and Edwards, 2000; this study), or 2) Au-bearing quartz (±carbonate, sulphide, Te-bearing minerals) vein systems cutting quartz diorite intrusions (e.g., McBride and Finlay McKinlay Au occurrences; Baldwin, 1987; Sherman et al., 1988, 1989; Sherman, 1992; Ferreira, 1993). In the southern belt, the Burnt Timber deposit is controlled mainly by chemical-structural traps (Yang and Beaumont-Smith, 2017) within the JSZ (Fedikow et al., 1991; Peck et al., 1998; Jones, 2005; Jones et al., 2006). The MacLellan and Gordon deposits in the northern belt of the LLGB are hosted in the regionally extensive Agassiz metallotect (Fedikow and Gale, 1982; Fedikow, 1986, 1992; Ma et al., 2000; Ma and Beaumont-Smith, 2001; Park et al., 2002; Yang and Beaumont-Smith, 2015a, 2015b, 2016). Detailed bedrock mapping is critical to understanding these differences in order to provide crucial constraints for the Au metallogeny of the LLGB and assistance for Au exploration in the belt.

This report presents new data on the geology, structure and metamorphism of the Gemmell Lake area; provides an updated geological and regional structural framework for the mapping area; and discusses implications for Au mineralization by the post-Sickle intrusive suite. The accompanying preliminary map (PMAP2019-2; Yang, 2019a) was created from 228 field stations, including 251 structural measurements collected in 2019 as well as compiled historical data (167 stations from Gilbert et al., 1980; 3 stations from Zwanzig et al., 1999; 131 stations from Beaumont-Smith, 2008; and a handful of historical drill data), and detailed airborne magnetic data kindly provided by Alamos Gold Inc.

Regional geology

The LLGB (Bateman, 1945) is endowed with various minerals, such as orogenic Au, magmatic Ni-Cu-Co and volcanogenic massive sulphide (VMS) Zn-Cu. It is a major tectonic element of the internal Reindeer zone of the Trans-Hudson orogen (Stauffer, 1984; Lewry and Collerson, 1990), which is the largest Paleoproterozoic orogenic belt of Laurentia (Hoffman, 1988; Corrigan et al., 2007, 2009; Corrigan, 2012). The belt is bounded to the north by the Southern Indian domain, composed of variably migmatitic metasedimentary rocks, various granitoids and minor metavolcanic and volcaniclastic rocks (Kremer et al., 2009; Martins et al., 2019). Synorogenic basins, including the Kisseynew metasedimentary domain, represent the southern limit of the LLGB (Gilbert et al., 1980; Fedikow and Gale, 1982; Syme, 1985; Zwanzig et al., 1999; Beaumont-Smith and Böhm, 2003, 2004; Zwanzig and Bailes, 2010). Paleoproterozoic greenstone belts with ages and lithological assemblages similar to the LLGB occur to the east (Rusty Lake belt), to the west (La Ronge belt) and to the far south (Flin Flon belt; e.g., Ansdell et al., 1999; Park et al., 2002; Ansdell, 2005; Corrigan et al., 2007, 2009, 2012; Glendenning et al., 2015; Hastie et al., 2018; Lawley et al., 2019).

The LLGB consists of two east-trending, steeply dipping belts that contain various supracrustal rocks, known locally as the Wasekwan group (Bateman, 1945; Gilbert et al., 1980), along with younger, molasse-type sedimentary rocks that constitute the Sickle group (Norman, 1933). The southern and northern belts are separated by granitoid plutons of the 1.89–1.87 Ga Pool Lake intrusive suite (Gilbert et al., 1980; Baldwin et al., 1987; Beaumont-Smith et al., 2006), which are further divided into pre- and post-Sickle intrusions based on their temporal relationships to the Sickle group. In the central and southern parts of the LLGB, the Sickle group overlies the Wasekwan group and felsic–mafic plutonic rocks of the Pool Lake intrusive suite along an angular unconformity (Gilbert et al., 1980). The Sickle group correlates well with the 1850–1840 Ma MacLennan group in the La Ronge greenstone belt of Saskatchewan in terms of lithological composition, stratigraphic position and contact relationships (Ansdell et al., 1999; Ansdell, 2005; Corrigan et al., 2009). Volcanic and plutonic rocks in the LLGB underwent peak metamorphism at 1.81–1.80 Ga. Cutting the entire LLGB are the much younger Mackenzie dikes (ca. 1267 Ma; Baragar et al., 1996), as indicated by regional aeromagnetic data.

Significant differences in the geology and geochemistry of the northern and southern belts in the LLGB may reflect regional differences in tectonic settings that were obscured by structural transposition and imbrication during multiple stages of deformation (Gilbert et al., 1980; Syme, 1985; Zwanzig et al., 1999). This complexity leads to the suggestion that the term 'Wasekwan group' should be abandoned because it contains disparate volcanic assemblages that were later structurally juxtaposed during the evolution of the LLGB (Zwanzig et al., 1999), and thus may represent a tectonic collage similar to that described in the Flin Flon belt (e.g., Stern et al., 1995). However, this report retains the term 'Wasekwan group' to maintain consistency with previous LLGB-related literature.

Geology of the Gemmell Lake area

The Gemmell Lake area, outlined in orange in Figure GS2019-2-1, is located in the southern belt of the LLGB and consists dominantly of the Wasekwan group supracrustal rocks intruded by plutons of the Pool Lake intrusive suite, which were unconformably overlain by the Sickle group epiclastic rocks (Figure GS2019-2-2; Yang, 2019a). Following the convention of previous workers (e.g., Beaumont-

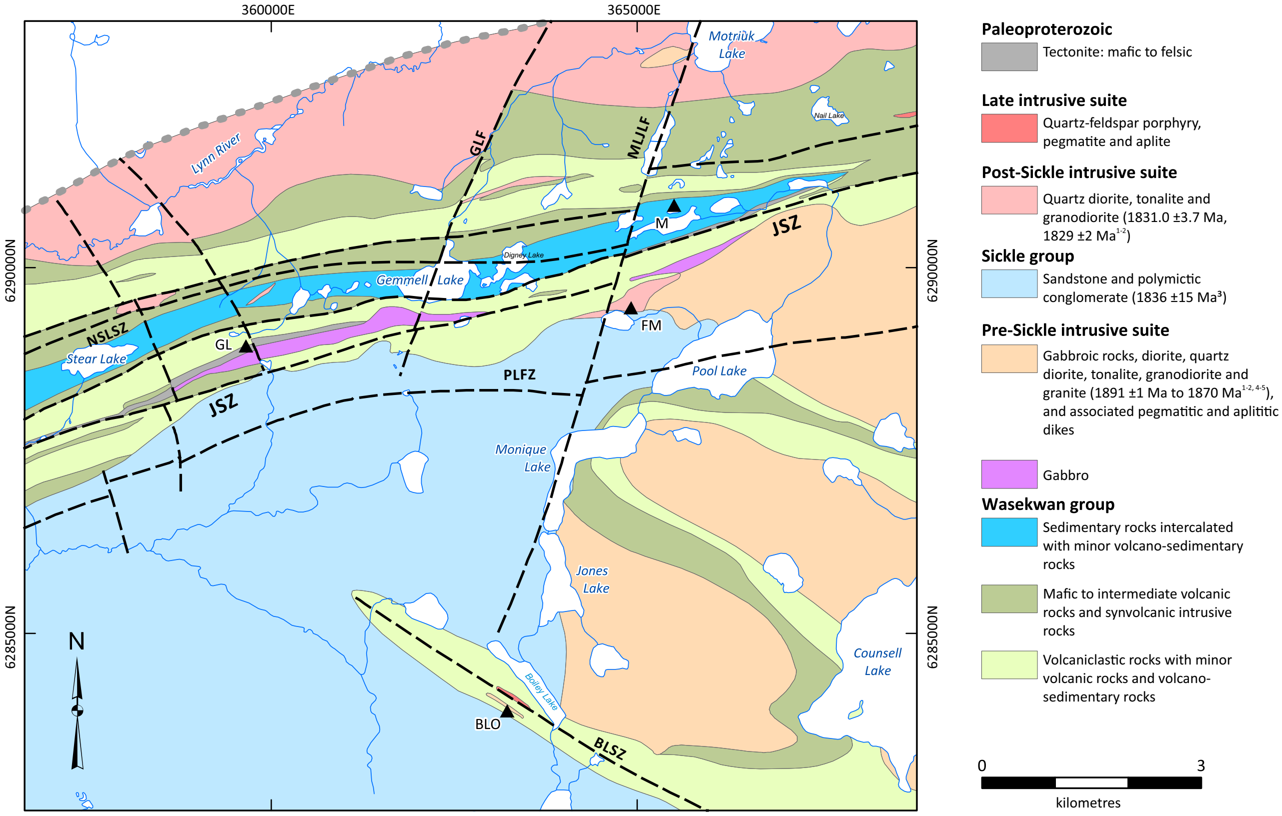

***Figure GS2019-2-2**: Simplified geology of the Gemmell Lake area, Lynn Lake greenstone belt, northwestern Manitoba (modified from Yang, 2019a). Black triangles indicate mineral occurrences: BLO, Boiley Lake Cu-(Au-Zn) occurrence; FM, Finlay McKinlay Au occurrence; GL, Gemmell Lake Au occurrence; M, McBride Au occurrence. Coarse dashed line indicates shear zone or fault: BLSZ, Boiley Lake shear zone; GLF, Gemmell Lake fault; JSZ, Johnson shear zone; MLJLF, Motriuk Lake–Jones Lake fault; NSLSZ, North Stear Lake shear zone; PLFZ, Pool Lake fault zone. Superscript numbers following U-Pb zircon ages in legend correspond to references in footnote of Table GS2019-2-1.*

Smith and Böhm, 2004), intrusions cutting the Wasekwan group (i.e., the Pool Lake intrusive suite of Gilbert et al., 1980) and those cutting the Sickle group are called, respectively, the pre-Sickle and post-Sickle (e.g., Milligan, 1960) suites; both are cut by a late intrusive suite, comparable to those identified in the areas of the MacLellan, Gordon and Burnt Timber Au mines (Yang and Beaumont-Smith, 2015a, b, 2017). Note that the structural terms used in this report follow those in Beaumont-Smith and Böhm (2003, 2004).

Nine map units comprising 18 subunits were defined during the course of bedrock mapping, which led to grouping into six affiliations: Wasekwan group, pre-Sickle intrusive suite, Sickle group, post-Sickle intrusive suite, late intrusive suite and tectonite (Table GS2019-2-1). These map units are described in the following sections and shown in Figure GS2019-2-2. The supracrustal rocks in the LLGB were mostly deformed and metamorphosed to greenschist and amphibolite facies (Gilbert et al., 1980; Beaumont-Smith and Böhm, 2004; Yang and Beaumont-Smith, 2015b, 2016, 2017); however, for brevity, this report omits the prefix 'meta'.

Wasekwan group (units 1 to 3)

Supracrustal rocks of the Wasekwan group exposed in the Gemmell Lake area are divided into the three units described below (see also Table GS2019-2-1).

Volcaniclastic rocks with minor volcanic rocks (unit 1)

Rocks of unit 1 are widespread in the central (e.g., north of Gemmell Lake), east-central (e.g., south of Pool Lake), southeastern (e.g., south of Boiley Lake) and western parts of the map area (Figure GS2019-2-2; Yang, 2019a). Covering a spectrum of rock types, unit 1 consists of mafic volcaniclastic rocks and intermediate–felsic volcanic and volcaniclastic rocks that, in places, appear to have been reworked by sedimentary processes. The volcaniclastic rocks of unit 1 include mafic breccia, tuff breccia, lapillistone, lapilli tuff and tuff; minor mafic mudstone and

Table GS2019-2-1: Lithostratigraphic units of the Gemmell Lake area, Lynn Lake greenstone belt, northwestern Manitoba

Unit[1]	Rock type	Affiliation
9	Tectonite: mafic to felsic	Tectonite
	Structural contact	
8	Quartz-feldspar porphyry, pegmatite and aplite	Late intrusive suite
	Intrusive contact	
7	Quartz diorite, tonalite and granodiorite (1831.0 ±3.7 Ma, 1829 ±2 Ma[2, 3])	Post-Sickle intrusive suite
7a	Quartz diorite, tonalite	
7b	Granodiorite	
	Intrusive contact	
6	Sandstone and polymictic conglomerate (1836 ±15 Ma[4])	Sickle group
6a	Arkosic sandstone and quartz pebbly sandstone	
6b	Polymictic conglomerate with minor pebbly sandstone	
	Unconformity	
5	Gabbroic rocks, diorite, quartz diorite, tonalite, granodiorite, and granite (1891 ±1 Ma to ~1870 Ma[2, 3, 5, 6]) and associated pegmatitic and aplitic dikes	Pre-Sickle intrusive suite
5a	Tonalite, granodiorite and granite, and associated pegmatitic and aplitic dikes	
5b	Diorite, quartz diorite and minor gabbroic rocks	
5c	Muscovite-bearing granite	
4	Gabbro	
	Intrusive contact	
3	Sedimentary rocks intercalated with minor volcanic sedimentary rocks	Wasekwan group
3a	Argillite, siltstone and greywacke	
3b	Banded iron formation	
3c	Volcanic mudstone, siltstone, sandstone and minor volcanic breccia	
	Structural contact	
2	Mafic–intermediate volcanic rocks and synvolcanic intrusive rocks	
2a	Diabase and gabbro	
2b	Porphyritic basaltic andesite	
2c	Plagioclase-phyric basalt and aphyric basalt	
2d	Pillow basalt	
	Structural contact	
1	Volcaniclastic rocks with minor volcanic rocks	
1a	Felsic–intermediate volcanic and volcaniclastic rocks	
1b	Intermediate lapilli tuff and tuff	
1c	Mafic lapillistone, mafic lapilli tuff, tuff, minor mafic mudstone and derivative garnet-biotite schist	
1d	Mafic tuff breccia and breccia	
	?	

[1] Yang (2019a)
[2] Beaumont-Smith and Böhm (2003)
[3] Turek et al. (2000)
[4] Lawley et al. (unpublished data, 2019)
[5] Baldwin et al. (1987)
[6] Yang and Lawley (2018)

intermediate to felsic lapilli tuff and tuff; and derivative garnet-biotite schist (e.g., south of Boiley Lake).

Outcrops of massive to foliated dacite and rhyolite (subunit 1a) with minor andesitic rocks and related volcaniclastic rocks are present in various places in the mapping area, and more abundant than similar rocks in the northern belt. Subunit 1a is exposed mainly in the central and west-central portions of the map area (Figure GS2019-2-2). These felsic–intermediate rocks are very fine grained, pale grey to white on weathered surfaces and light to medium greyish red or grey on fresh surfaces. Primary features (i.e., flow banding, porphyritic texture) are preserved despite these rocks being foliated and recrystallized (Figure GS2019-2-3a). Porphyritic dacite and rhyolite contain equant or subrounded quartz (1–2 mm) and locally subhedral to euhedral feldspar (0.5–1.5 mm) phenocrysts embedded in a very fine grained to aphanitic groundmass. Locally, very fine grained dark grey bands (up to 1 cm) alternate with pale to light reddish felsic bands, forming flowbanding. In ductile-brittle shear zones, these rocks are commonly mylonitized, and silicified and sericitized, locally containing scattered pyrite (and arsenopyrite, ±chalcopyrite) disseminations. Some of them are likely Au bearing, forming Au occurrences such as at Gemmell Lake. Boudinaged vein quartz occurs in some outcrops along the main S_2 foliation planes, some of it containing fine-grained pyrite.

Intermediate lapilli tuff and tuff (subunit 1b) typically display millimetre- to centimetre- scale layers, interpreted to represent beds even though they are foliated and locally folded. Lapilli tuff contains elongated lithic fragments (up to 6 cm in length) of variable composition (e.g., rhyolite, porphyritic andesite, aphanitic basalt) that are embedded in a fine-grained matrix consisting of amphibole, biotite, chlorite, epidote, plagioclase and aphanitic material. Alternating ~0.5–1 cm thick, dark grey and pale yellow-grey layers are common and interpreted to represent mafic and intermediate–felsic intercalations. Lapilli tuff appears to grade laterally to fine-grained tuff that contains interbedded mafic and felsic laminae (~0.5–2 mm), and in which larger lapilli-sized lithic fragments are rare or absent. Some tuff and lapilli tuff are moderately to strongly magnetic due to the presence of scattered, euhedral to subhedral magnetite porphyroblasts (up to 1%; 0.5–2 mm). Noteworthy are plagioclase crystal tuff and lapilli tuff, with thin felsic layers up to 1 cm thick (Figure GS2019-2-3b) that contain up to 10% plagioclase fragments of varied shape (e.g., angular, irregular), ranging in size from 0.1 to 20 mm and unevenly distributed at the outcrop scale. This feature distinguishes the plagioclase crystal tuff and lapilli tuff from plagioclase-phyric basalt and basaltic andesite (see subunit 2b and 2c described below). Subunit 2a diabase and/or gabbroic dikes cut laminated andesitic tuff and lapilli tuff (Figure GS2019-2-3c).

Mafic volcaniclastic rocks are grouped into two subunits: subunit 1c consists of lapillistone, lapilli tuff, tuff, minor mafic mudstone and derivative garnet-biotite schist, whereas subunit 1d consists mainly of mafic tuff breccia and breccia (Table GS2019-2-1). Mafic lapillistone, lapilli tuff and tuff (subunit 1c) are characterized by the presence of mafic lithic fragments in a chloritic matrix. Minor greenish grey, very fine grained, thinly bedded mafic mudstone is also included in subunit 1c, which usually weathers light greenish brown to light grey and contains disseminated pyrrhotite and pyrite. Dark green, acicular amphibole (actinolite?) porphyroblasts (up to 5–10 mm), concentrated in foliation or fracture planes in mafic tuff and lapilli tuff, are interpreted to have formed by retrograde metamorphism to greenschist facies. The mafic lapilli tuff and tuff (subunit 1c) are generally moderately to strongly foliated and range from texturally variable to relatively homogeneous. These rocks consist of varied amounts of aphyric lithic fragments, plagioclase (up to 40%; 0.1–5 mm) and chloritic amphibole pseudomorphs after pyroxene (up to 15%; 0.2–12 mm) in a fine-grained mafic-tuff matrix. Magnetite and amphibole porphyroblasts are evident in places. Mafic lapilli-sized fragments make up <25% of subunit 1c but can locally account for up to 80% of the rocks, which are then termed mafic lapillistone.

Garnet-biotite schist of subunit 1c occurs mainly close to the contact zone of a muscovite-bearing granite dike (subunit 5c; see below) with mafic mudstone and tuff to lapilli tuff, south of Boiley Lake, where the northwest-trending Boiley Lake shear zone cuts through these rock units. The garnet-biotite schist is composed of biotite, plagioclase, garnet, chlorite, quartz and minor magnetite. Relicts of lithic fragments and rotated garnet porphyroblasts (up to 2.2 cm) are locally evident along S_2 foliation planes (Figure GS2019-2-3d). More complex metamorphic-mineral assemblages present in the schist were reported previously, including garnet-chlorite±magnetite, garnet-anthophyllite-chlorite-magnetite and kyanite-muscovite-biotite-chlorite (Anderson and Beaumont-Smith, 2001; Assessment File 92793, Manitoba Agriculture and Resource Development, Winnipeg). This schist constitutes the Boiley Lake alteration zone (Gale, 1983; Ferreira, 1993), which likely resulted from contact and/or regional metamorphism of hydrothermally altered volcaniclastic to volcanic sedimentary rocks (Anderson and Beaumont-Smith, 2001). Similar garnet-biotite schist containing minor magnetite porphyroblasts is also present east of Digney Lake, where it occurs close to the contact of a gabbro (unit 4) intrusion emplaced into the unit 1 volcaniclastic rocks.

Subunit 1d consists of moderately to strongly deformed and foliated heterolithic mafic tuff breccia and breccia. Lithic fragments, ranging from 8 to 25 cm in length, include plagioclase-phyric basalt, plagioclase-amphibole–phyric basalt, aphyric basalt, lapilli tuff, very fine grained andesite and minor rhyolite clasts embedded in a lapilli tuff and tuff matrix (Figure GS2019-2-3e). The basaltic fragments are subrounded to subangular, varying in shape from irregular to rarely ellipsoidal, and have been stretched along the generally east- to southeast-trending foliation (S_2). In high-strain zones, lithic fragments are

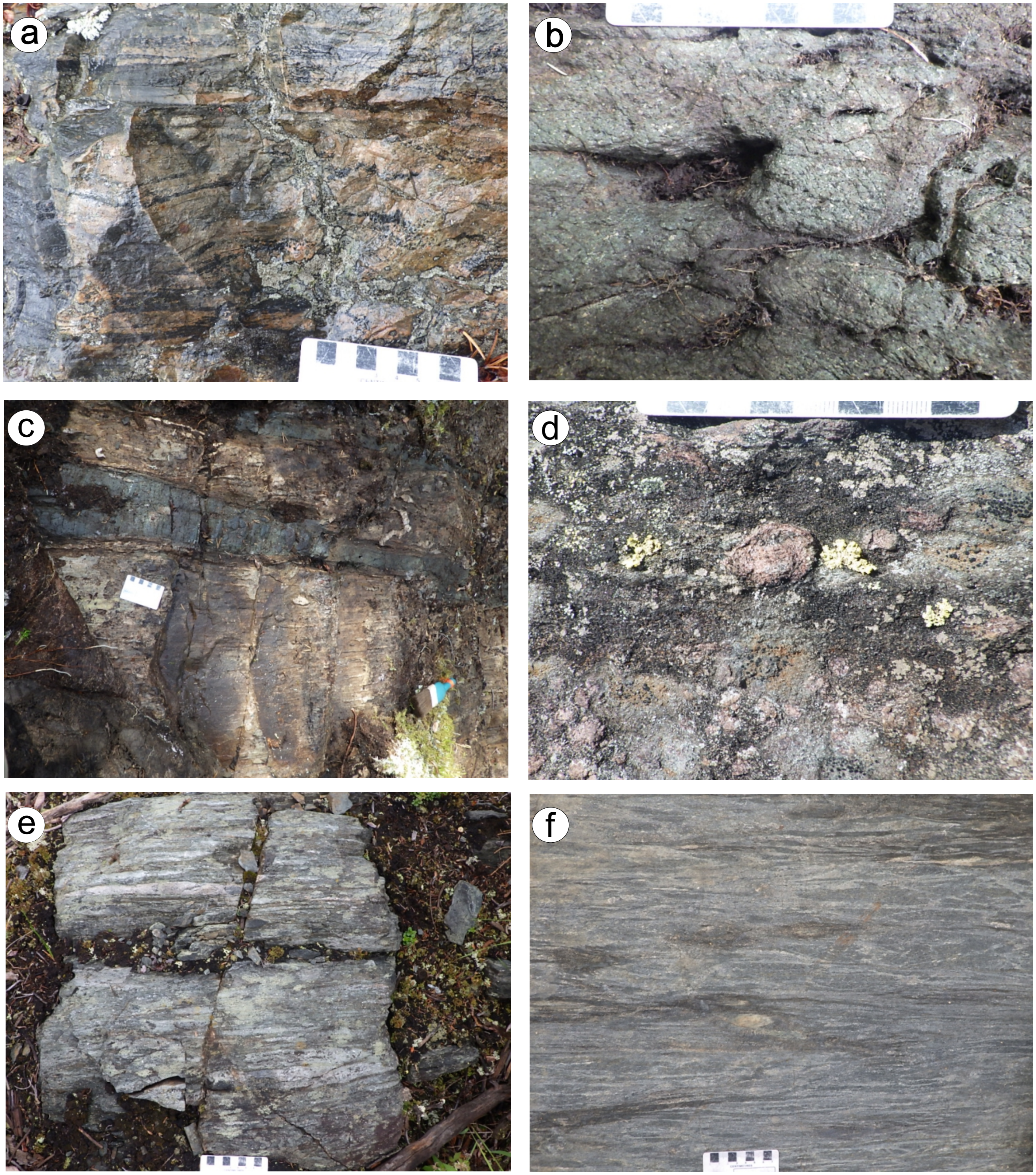

Figure GS2019-2-3: *Field photographs of unit 1 volcaniclastic rocks with minor volcanics of the Wasekwan group in the Gemmell Lake area:* ***a)*** *very fine grained quartz- and feldspar-phyric rhyolite with flow bands, and locally felsic fragments (subunit 1a; UTM Zone 14N, 361000E, 6288737, NAD 83);* ***b)*** *intermediate tuff to lapilli tuff (with up to 10% 0.2–1.5 mm plagioclase fragments) with rare lithic fragments (subunit 1b; UTM 357536E, 6288334N);* ***c)*** *laminated andesitic tuff to lapilli tuff (subunit 1b) cut by a diabase dike (subunit 2a; UTM 363174E, 6291169N);* ***d)*** *garnet-biotite schist with reddish garnet porphyroblasts, up to 2 cm (centre of photo), that are rotated clockwise due to dextral shear along S_2 foliation (subunit 1c; UTM 363432E, 6284030N);* ***e)*** *foliated mafic tuff breccia and breccia with basaltic to andesitic fragments transposed along S_2 foliation (subunit 1d; UTM 364998E, 6288128N);* ***f)*** *very strongly foliated basaltic tuff breccia in high-strain zone (subunit 1d; UTM 357722E, 6287441N).*

sheared and flattened, although the margins of some of the fragments are still discernible (Figure GS2019-2-3f). Some of the aphanitic basalt fragments display epidote alteration and others show reaction rims with very fine grained assemblages of chlorite, epidote, sericite and albite. Some porphyritic basalt blocks contain well-preserved plagioclase and amphibole (after pyroxene) phenocrysts.

Mafic to intermediate volcanic rocks and synvolcanic intrusive rocks (unit 2)

Unit 2 mafic to intermediate volcanic rocks occur mainly in the northeastern (e.g., Nail Lake), northern, east-central (e.g., south of Poll Lake) and southeastern (e.g., south of Monique Lake) parts of the map area (Figure GS2019-2-2). The volcanic succession of unit 2 in the Gemmell Lake area is dominated by plagioclase-phyric and aphyric basalts and pillow basalts, with subordinate porphyritic basaltic andesite and synvolcanic diabase and gabbro dikes (Table GS2019-2-1).

Synvolcanic diabase and gabbroic rocks (subunit 2a) usually occur as dikes and small plugs intruded into unit 2 volcanic rocks (Figure GS2019-2-4a) and, in some cases, into unit 1 volcaniclastic rocks (Figure GS2019-2-3c). The diabase dikes weather greenish grey to grey and are greenish to dark green on fresh surfaces; they are very fine to medium grained, porphyritic and moderately to strongly foliated (Figure GS2019-2-4b). Equant to subhedral plagioclase phenocrysts (up to 10 mm) occur in a fine-grained groundmass of plagioclase, amphibole, chlorite and Fe oxides. Generally, the diabase and gabbroic rocks consist of 50–60% amphibole and 40–50% plagioclase, reflecting an amphibolite-facies metamorphic-mineral assemblage. Grain boundaries between the phenocrysts and groundmass are diffuse due to sericite and chlorite alteration, regardless of the extent of deformation. Trace disseminated sulphides (e.g., pyrrhotite; ~0.5–1 mm) are locally evident.

Porphyritic basaltic andesite (subunit 2b) contains amphibole (±biotite) and lesser amounts of plagioclase phenocrysts in a fine-grained groundmass (Figure GS2019-2-4c), although, in some cases, it lacks plagioclase phenocrysts. Biotite and sericite alteration is a common feature of the rock. When plagioclase and amphibole phenocrysts coexist in basaltic andesite (subunit 2b), it is difficult to distinguish it from plagioclase-phyric basalt (subunit 2c), although the latter commonly lacks amphibole (±biotite) phenocrysts (Figure GS2019-2-4d, e).

Massive aphyric basalt (subunit 2c) is also common in the map area. Vesicles and quartz±calcite amygdules are present in some outcrops. The basalt is greyish green on weathered surfaces and dark greyish green on fresh surfaces. In most cases, it is aphanitic. Chlorite and epidote alteration is common in the aphyric basalt, as shown by epidote domains ranging from a few centimetres to a metre across. These epidote domains are generally irregular to ovoid, displaying sharp to gradational contacts with the host aphyric basalt, although some epidote is fracture controlled as veins or veinlets, similar to those described by Gilbert et al. (1980), Gilbert (1993) and Yang and Beaumont-Smith (2016, 2017).

Pillowed basalt (subunit 2d) is exposed and well preserved in a relatively low-strain area along the southern shore of Pool Lake (Figure GS2019-2-2). Pillow size ranges from 20 to 40 cm (Figure GS2019-2-4f) and locally reaches up to 150 cm, with well-preserved hyaloclastite selvages up to 3 cm thick. Locally, subrounded to rounded quartz±carbonate amygdules up to 1.0 cm in diameter are concentrated along the inner margin of pillow selvages. In high-strain areas, pillows are strongly deformed and contain a penetrative foliation, with width to length ratios of the flattened pillows being up to 1:10. Some pillow selvages are still recognizable and contain stretched vesicles and quartz amygdules transposed along S_2 foliation. Epidote alteration as veinlets, patches or nodules was commonly observed in the basalt with few plagioclase phenocrysts. Late quartz veins occur either along or cutting S_2 foliation planes; some are boudinaged or folded.

Sedimentary rocks intercalated with minor volcanic sedimentary rocks (unit 3)

Unit 3 sedimentary rocks of the Wasekwan group are subordinate to volcanic and volcaniclastic rocks in the map area. The sedimentary rocks are exposed mainly in the central and southwestern portions of the map area (Figure GS2019-2-2). This unit consists of argillite, siltstone and greywacke (subunit 3a), and banded iron formation (BIF; subunit 3b), intercalated with minor volcanic mudstone, siltstone, sandstone and breccia (subunit 3c) (Table GS2019-2-1).

Thin- to medium-bedded quartzofeldspathic greywacke and siltstone (subunit 3a) dominate the sedimentary succession. Greywacke contains more than 15% clay minerals in its matrix. Primary bedding (S_0) in the sedimentary rocks was transposed by the regional S_2 foliation. The medium- to coarse-grained greywacke is medium tan to yellowish grey on weathered surfaces, and light grey on fresh surfaces. Quartz, feldspar, amphibole and lithic clasts (1.3–2 mm) are angular to subrounded, and well aligned on foliation planes defined by biotite flakes and manifested by felsic- and mafic-rich layering that is likely to reflect transposed bedding (Figure GS2019-2-5a).

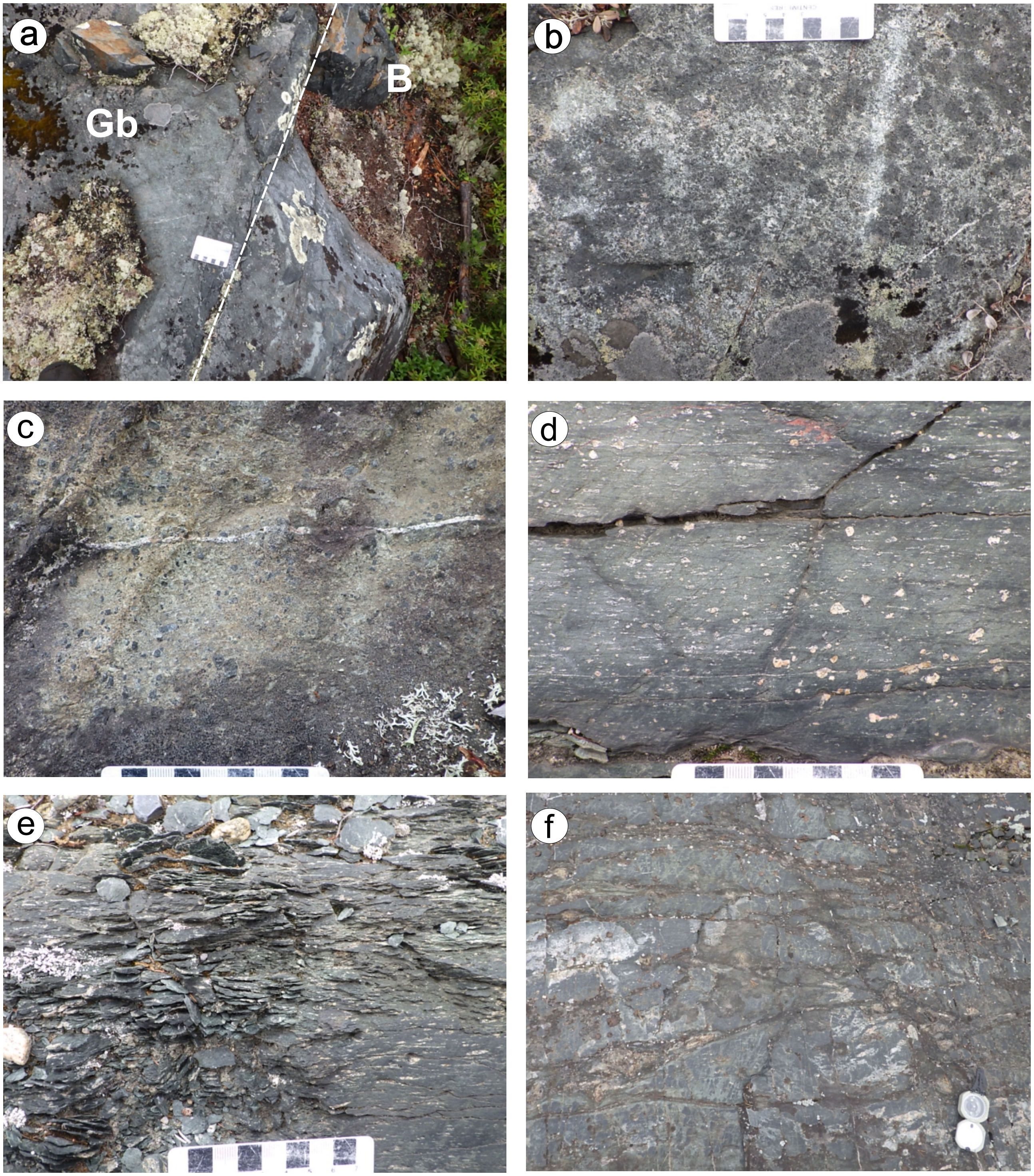

Figure GS2019-2-4: *Field photographs of mafic to intermediate volcanic rocks and synvolcanic intrusive rocks (unit 2) of the Wasekwan group in the Gemmell Lake area:* ***a)*** *synvolcanic, massive gabbro (subunit 2a) cuts very fine grained aphyric basalt (subunit 2c; UTM Zone 14N, 366090E, 6288191N, NAD 83);* ***b)*** *massive gabbro with subhedral to euhedral plagioclase laths in very fine grained mafic groundmass (subunit 2a; same location as photo a);* ***c)*** *amphibole-phyric basaltic andesite (subunit 2b; UTM 368905E, 6292155N);* ***d)*** *foliated plagioclase-phyric basalt (subunit 2c; UTM 357621E, 6287253N);* ***e)*** *strongly foliated plagioclase-phyric basalt (subunit 2c; UTM 357621E, 6287253N);* ***f)*** *foliated pillow basalt with well-preserved hyaloclastite selvage up to 3 cm thick; the stretched pillows are aligned along east-trending S_2 foliation planes (subunit 2d; UTM 365139E, 6288262N). Abbreviations: B, basalt; Gb, gabbro.*

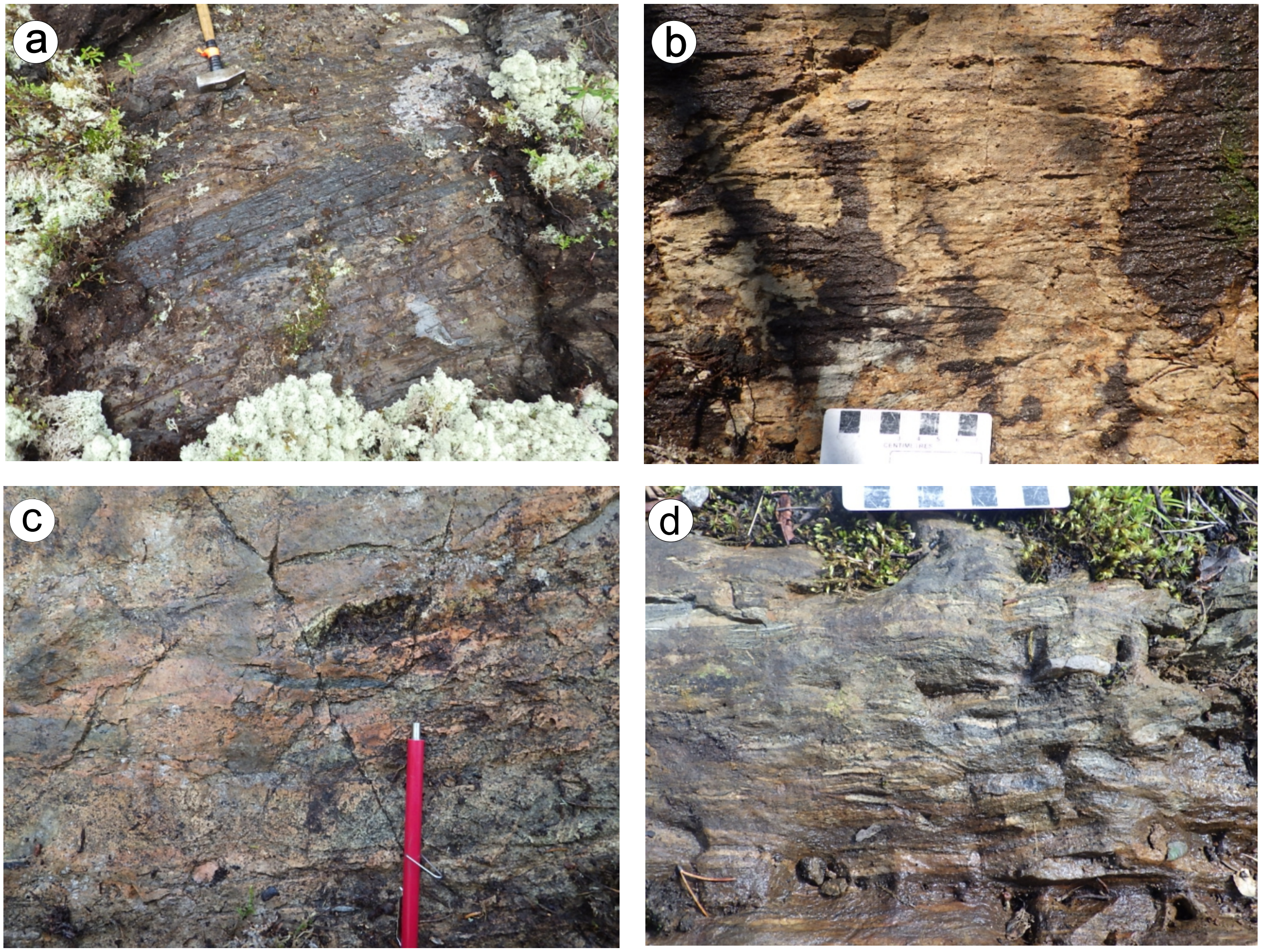

Figure GS2019-2-5: *Field photographs of sedimentary rocks intercalated with minor volcano-sedimentary rocks (unit 3) of the Wasekwan group in the Gemmell Lake area:* ***a)*** *fine- to medium-grained, foliated quartzofeldspathic greywacke with alternating felsic and mafic bands or layering (subunit 3a; UTM Zone 14N, 359742E, 6289520N, NAD 83);* ***b)*** *laminated volcanic (andesitic) sandstone with biotite flakes and plagioclase clasts (0.5–2 mm) that have diffuse margins (subunit 3c; UTM 364058E, 6290114N);* ***c)*** *volcanic sandstone containing disseminated magnetite, as well as magnetite aggregates up to 10 cm in length (subunit 3c; UTM 363996E, 6289919N);* ***d)*** *volcanic breccia with felsic and mafic volcanic fragments in a felsic to intermediate sandy matrix; bedding transposed by S_2 foliation (subunit 3c; UTM, 364850E, 6290199N).*

Scattered sulphide minerals dominated by pyrite are evident in the greywacke; in many cases, they are associated with quartz veins and veinlets. Low-strain domains show millimetre- to centimetre-thick beds indicated by dark green mafic to light tan felsic layers.

Although no BIF (subunit 3b) was found at exposed outcrops during the course of mapping, it was intersected by a number of historical drill holes in the central, northeastern and southwestern parts of the map area. The BIF is well correlated with highly magnetic, east-northeast-trending domains indicated by detailed airborne magnetic surveys, and consistently overlies unit 2 mafic–intermediate volcanic rocks.

Thin to thick beds of minor volcanic sedimentary rocks (subunit 3c), present in the upper section of unit 3, consist of volcanic mudstone, siltstone and sandstone, and minor volcanic breccia (Table GS2019-2-1). Volcanic sandstone is dominated by laminated, fine- to medium-grained andesitic sandstone consisting mainly of irregular plagioclase, biotite flakes and lithic fragments (0.5–2 mm) in a fine sandy matrix; locally, a few large lithic fragments occur along bedding transposed by regional S_2 foliation (Figure GS2019-2-5b). Recrystallized acicular amphibole crystals (actinolite; up to 1.5 cm in length) are randomly oriented along S_2 planes in the andesitic sandstone, indicating that it experienced greenschist-facies retrograde metamorphism (Yang and Beaumont-Smith, 2017). Locally, subunit 3c volcanic sandstone contains ~1% cubic magnetite grains (0.2–0.3 mm), as well as magnetite fragments (~0.5 cm wide) up to 10 cm in length (Figure GS2019-2-5c). Similar volcanic sedimentary rocks occur west of Wasekwan Lake (Yang and Beaumont-Smith, 2017).

Thick-bedded volcanic breccia (a minor component of subunit 3c) at the base of unit 3 consists dominantly of felsic and intermediate–mafic volcanic clasts in a coarse-grained sandy matrix (Figure GS2019-2-5d). These clasts are stretched or flattened and well aligned along S_2 planes that transposed primary bedding. Although strongly deformed, the breccia appears to grade upward to volcanic sandstone, suggesting that the beds young to the north.

Pre-Sickle intrusive suite (units 4 and 5)

Rocks of the pre-Sickle intrusive suite crosscut the supracrustal rocks of the Wasekwan group (Gilbert et al., 1980; Baldwin et al., 1987; Beaumont-Smith and Bohm, 2004). Unit 4 gabbro and unit 5 granitoid rocks, diorite, quartz diorite and minor gabbroic rocks were attributed to this suite (Table GS2019-2-1).

Gabbro (unit 4)

Gabbro of unit 4 occurs mainly in the central to southwestern part of the Gemmell Lake area (Figure GS2019-2-2). It occurs as a sill-like intrusion cutting the Wasekwan group supracrustal rocks, and is cut by unit 5 granitoids. The gabbro weathers greenish grey and is dark greenish grey to dark grey on fresh surfaces. It is medium to coarse grained, equigranular, massive, and moderately to locally strongly foliated. It consists of 30–40% plagioclase laths (1–3 mm), 55–60% amphibole (pseudomorphs after pyroxene), minor Fe-oxide minerals and trace pyrrhotite (Figure GS2019-2-6a). The edges of both plagioclase and amphibole crystals are diffuse due to chlorite and sericite alteration. Locally, epidote veins and veinlets up to 4 cm wide are evident along S_2 planes.

Granitoid rocks (subunit 5a)

Granitoid plutons of the pre-Sickle intrusive suite (unit 5), exposed in the southeastern and southern parts of the map area (Figure GS2019-2-2), comprise diorite, quartz diorite, tonalite, granodiorite, granite and associated pegmatitic and aplitic dikes, as well as minor gabbroic rock. These intrusive rocks are divided into three subunits based on field relations and lithology: 1) tonalite, granodiorite and granite, and associated pegmatitic and aplitic rocks (subunit 5a); 2) diorite, quartz diorite and minor gabbroic rocks (subunit 5b); and 3) muscovite-bearing granite (subunit 5c; Table GS2019-2-1).

Subunit 5a granodiorite is commonly medium to coarse grained, massive, equigranular to locally porphyritic and weakly to moderately foliated. It weathers greyish pink to light beige and consists of 20–30% anhedral quartz, 25–35% subhedral plagioclase, 20–25% K-feldspar, 5–10% hornblende±biotite, and accessory Fe-oxide minerals. Some of the porphyritic variety contains 5% quartz phenocrysts up to 1.2 cm across (Figure GS2019-2-6b), suggesting relatively shallow emplacement into the Wasekwan group supracrustal package. Less commonly, granite of subunit 5a contains slightly higher K-feldspar and quartz contents than the granodiorite, whereas tonalite of subunit 5a is relatively enriched in plagioclase and hornblende, and lacks (or has <10%) K-feldspar. Pegmatite and/or aplite of unit 5a are more commonly associated with granite and granodiorite than with tonalite. They occur as dikes that are a few centimetres to a few metres wide and consist of quartz, feldspar and minor biotite (±muscovite).

Diorite, quartz diorite and minor gabbroic rocks (subunit 5b)

Diorite and quartz diorite (subunit 5b) occur mostly as marginal phases of the Counsell Lake pluton in the southern part of the map area (Figure GS2019-2-2). Quartz diorite is fine to medium grained, massive, equigranular and moderately to strongly foliated. It consists of 5–10% anhedral quartz, 50–60% plagioclase with diffuse grain boundaries, 20–30% hornblende, and minor biotite. Where the rock lacks quartz or contains <5% quartz, it is termed diorite.

An outcrop (~15 m across) southwest of Motriuk Lake displays a cumulate-layering texture with variations in mineral-grain size and percentage from base to top. This sequence consists of megacrystic pyroxenite to melagabbro grading to very coarse grained pyroxenite to melagabbro, coarse- to medium-grained gabbro and fine- to medium-grained quartz diorite, all of which are cut by pinkish pegmatite dikes. The megacrystic phase is dark grey, massive and equigranular, and composed of 85–90% euhedral cumulus pyroxene (up to 2 cm) and 10–15% anhedral to subhedral plagioclase interstitial to the former (Figure GS2019-2-6c). Very coarse grained pyroxenite to melagabbro comprises similar minerals, also exhibiting cumulate texture (Figure GS2019-2-6d), and grades into gabbro containing about 60–80% pyroxene and 20–40% plagioclase. The contact between the mafic rocks and quartz diorite (Figure GS2019-2-6e) is gradational at the outcrop scale, suggesting that they formed by fractional crystallization from the same magmatic system.

Muscovite-bearing granite (subunit 5c)

Muscovite-bearing granite of subunit 5c is only exposed immediately southwest of Boiley Lake (Figure GS2019-2-2), where it occurs as a dike-like intrusion up to 20 m wide cutting unit 1 volcanic to volcaniclastic rocks. Its southwestern margin is strongly sheared and

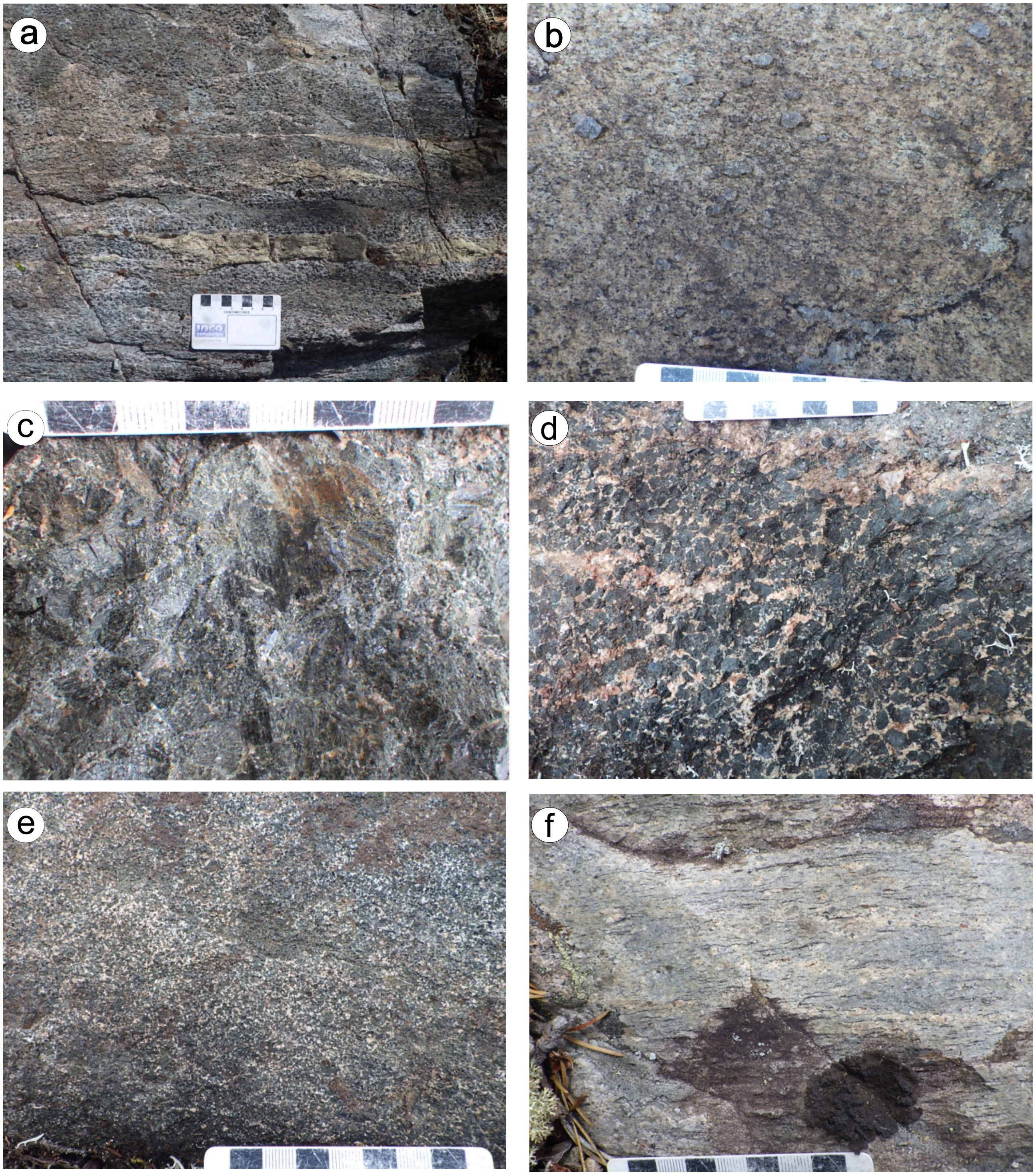

Figure GS2019-2-6: *Outcrop photographs of units 4 and 5 in the Gemmell Lake area:* ***a)*** *foliated, massive, medium- to coarse-grained equigranular gabbro with epidote veinlets and veins up to 4 cm wide present along S_2 planes (unit 4; UTM Zone 14N, 361527E, 6289275N, NAD 83);* ***b)*** *foliated, medium- to coarse-grained porphyritic granodiorite with quartz phenocrysts (2–5 mm; subunit 5a; UTM 365201E, 6283371N);* ***c)*** *megacrystic pyroxenite to melagabbro and* ***d)*** *massive, very coarse grained pyroxenite to melagabbro with cumulate texture, cut by pegmatitic veins (and dike; not shown; subunit 5b; UTM 365566E, 6293020N);* ***e)*** *massive, fine- to medium-grained quartz diorite (subunit 5b; UTM 3655666E, 6293020N);* ***f)*** *foliated, porphyritic muscovite-bearing granite (subunit 5c) with K-feldspar and quartz phenocrysts in felsic groundmass consisting of quartz, feldspar, biotite and muscovite, intruding unit 1 volcaniclastic and volcanic sedimentary rocks (UTM 363298E, 6283932N); note that magnetite-garnet-biotite schist occurs in the contact zone between two-mica granite and unit 1 volcaniclastic rock and volcanic mudstone.*

becomes protomylonitic to mylonitic in contact with the subunit 1c garnet-biotite schist. This light grey granite is fine to medium grained and massive to locally porphyritic but strongly foliated, as indicated by biotite aligned along S_2 foliation (Figure GS2019-2-6f). Potassium feldspar phenocrysts with diffuse grain boundaries are also aligned along the foliation. Typically, the granite contains ~0.5% muscovite flakes (0.2–0.5 mm across) evenly distributed with 25–35% quartz, 55–60% feldspars and 5–6% biotite. This two-mica granite is likely an S-type granite in terms of its mineral assemblage and formed in relatively reducing conditions.

Sickle group (unit 6)

Sickle group sandstone (subunit 6a) and polymictic conglomerate (subunit 6b), which outcrop in the central and southwest-central parts of the map area (Figure GS2019-2-2), unconformably overlie the Wasekwan group supracrustal rocks as well as the pre-Sickle intrusive rocks. Stratigraphically, sandstone overlies conglomerate (Norman, 1933; Gilbert et al., 1980). A maximum depositional age of 1836 ±15 Ma for the Sickle group was recently obtained from the youngest, reproducible detrital zircon grain retrieved from a quartz pebbly sandstone sample collected west of Pool Lake (Lawley et al., unpublished data, 2019).

Arkosic sandstone and quartz pebbly sandstone (subunit 6a)

Medium- to thick-bedded arkosic sandstone and quartz pebbly sandstone display varied colours on fresh surface, including pale grey, dark grey and tan to light reddish. The sandstones are fine to coarse grained and are composed of feldspar, quartz, mica, lithic fragments and finer material. Up to 10% quartz pebbles (3–5 mm) are common in the quartz pebbly sandstone (Figure GS2019-2-7a), together with sand- to pebble-sized feldspar clasts. Locally, variation in grain size may indicate the top of sandy beds, although this subunit was deformed and foliated by the extensive D_2 deformation that resulted in the transposition of primary bedding (S_0) along the S_2 foliation. In places, arkosic sandstone contains more pebbly lithic clasts (up to 15 mm) in a finer matrix of feldspar, quartz, mica, chlorite, magnetite and clays. Arkose to arenite lacking quartz or lithic pebbles is exposed west of Jones Lake.

Polymictic conglomerate with minor pebbly sandstone (subunit 6b)

In domains of low- to moderate-strain, the polymictic conglomerate (subunit 6b) is poorly sorted and matrix to clast supported, and contains varied sizes (2–30 cm) of rounded and subrounded to irregular clasts ranging from pebble to boulder size. Generally, cobble-size clasts are more common. Clast types include mafic–felsic volcanic rocks, granitoids, vein quartz, epidotized fragments, magnetic BIF and chert in a sandy to wacke matrix (Figure GS2019-2-7b, c). Some of the matrix contains sand-sized K-feldspar, biotite, muscovite, chlorite and magnetite grains. In high-strain domains, conglomerate displays strong clast flattening and stretching along the S_2 foliation (Figure GS2019-2-7d) that entirely transposed bedding (S_0). Locally, medium- to thin-bedded pebbly sandstone to coarse-grained arkosic sandstone is interbedded with polymictic conglomerate.

Post-Sickle intrusive suite (unit 7)

Post-Sickle intrusive rocks of unit 7, represented by the Motriuk Lake pluton, occur dominantly in the northern part of the map area, and a few dikes and stock-like intrusions cut the Wasekwan group rocks southwest of Gemmell Lake (Figure GS2019-2-2). This unit comprises two subunits: quartz diorite and tonalite (subunit 7a) and granodiorite (subunit 7b) (Table GS2019-2-1). Quartz diorite is medium to coarse grained, massive, weakly to moderately deformed and equigranular, although porphyritic texture is locally evident. It is composed of 5–10% quartz, 60–70% plagioclase and 15–20% amphibole (Figure GS2019-2-8a). Quartz diorite and tonalite of the Motriuk Lake pluton (Yang and Beaumont-Smith, 2015a) in the current map area coincide with magnetic lows on detailed airborne magnetic imagery. The rocks have high Sr/Y and La/Yb ratios (Yang, unpublished data, 2015), similar to those of post-Sickle quartz diorite at Farley Lake that exhibits geochemical characteristics of adakite-like rocks (see Yang and Lawley, 2018).

Granodiorite of subunit 7b is pinkish on fresh surfaces and weathers beige to tan, and is medium to coarse grained, foliated and equigranular to locally porphyritic. It consists of 5–8% hornblende (partly altered to biotite), 3–5% discrete biotite flakes, 25–30% quartz, 30–40% plagioclase and 25–30% K-feldspar.

Late intrusive suite (unit 8)

Unit 8 quartz-feldspar porphyry, pegmatite and/or aplite occur mostly as dikes in the southwestern and northeastern portions of the map area (Figure GS2019-2-2). These dikes tend to be isolated, relatively less deformed and apparently not associated with any of the larger intrusions mapped at surface. Unit 8 intrusives have an unclear relationship to the pre- and post-Sickle intrusive suites (unit 5 and unit 6, respectively) and are therefore ascribed to the late intrusive suite. A quartz-feldspar porphyry dike

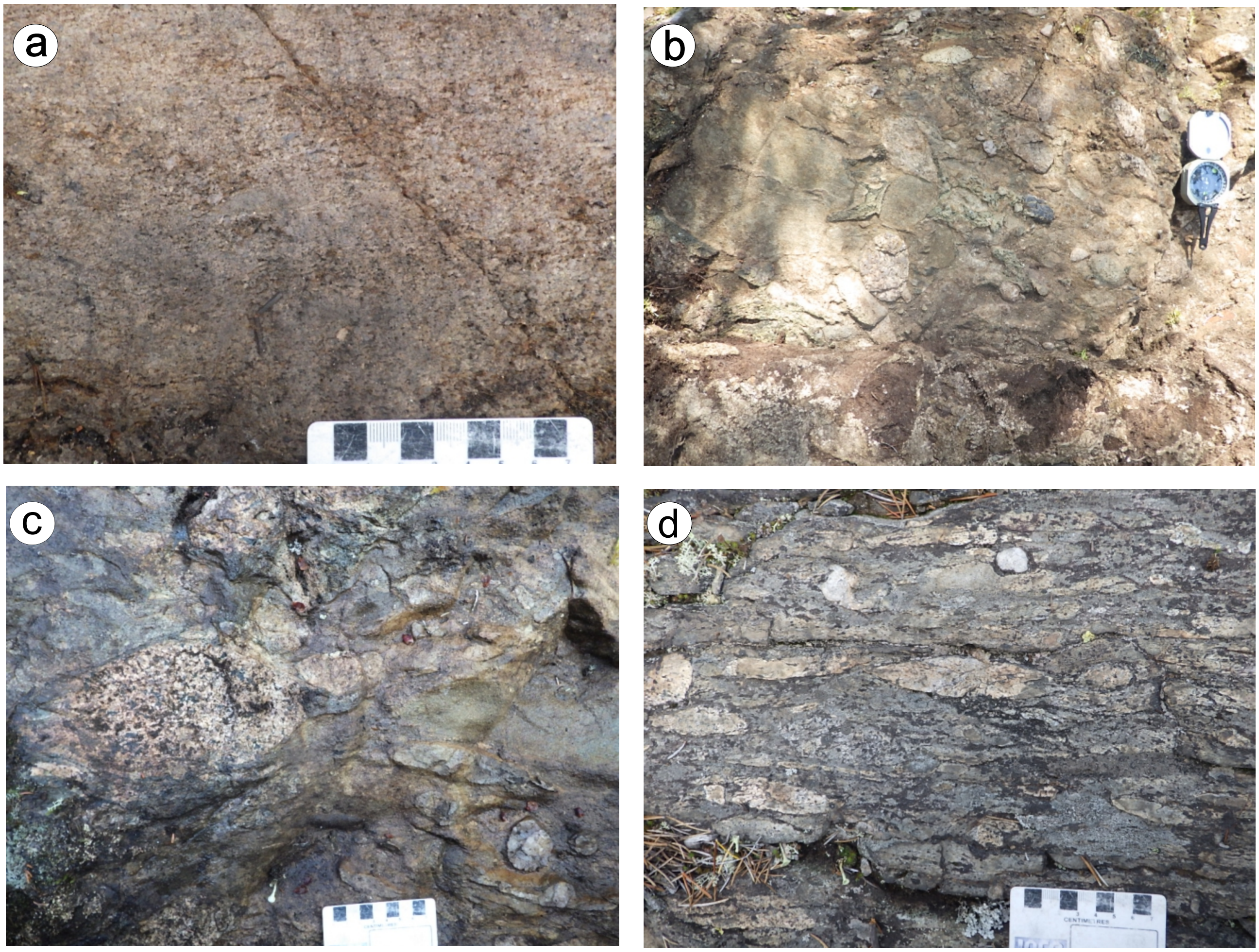

***Figure GS2019-2-7:** Outcrop photographs of unit 6 Sickle group sandstone and polymictic conglomerate in the Gemmell Lake area: **a)** quartz pebbly arkosic sandstone (subunit 6a; UTM Zone 14N, 3639917E, 6287707N, NAD 83); **b)** poorly sorted, polymictic cobble conglomerate with wacke matrix and variously shaped clasts consisting of granitoid, vein quartz, banded iron formation, chert and felsic and mafic volcanic rocks, together with a few irregular felsic boulder-sized clasts (subunit 6b; UTM 364101E; 6286914N); **c)** weakly foliated, matrix- to clast-supported, poorly sorted, polymictic pebble to cobble conglomerate with sandy matrix (subunit 6b; UTM 365031E; 6289411N); **d)** strongly foliated polymictic conglomerate with stretched granitoid, rhyolite, chert and banded iron formation clasts and subrounded quartz clasts, aligned along S_2 foliation planes that transposed S_0 bedding (subunit 6b; UTM 363910E; 6287957N).*

(up to 10 m wide) south of Boiley Lake contains ~2% magnetite phenocrysts that are cubic to subhedral (1–3 mm), together with quartz and K-feldspar embedded evenly in a felsic groundmass (Figure GS2019-2-8b). The presence of magnetite phenocrysts indicates that the dike may have formed in relatively oxidized conditions. Hydrothermal fluids associated with such oxidized intrusion(s) can effectively scavenge and transport gold (e.g., Boyle, 1979), and thus may have played a role in Au mineralization.

Unit 8 pegmatite and aplite commonly have muscovite (±tourmaline) in addition to biotite, suggesting that they are likely not related to the pre-Sickle (subunit 5) and post-Sickle (subunit 7) intrusive suites (Yang and Beaumont-Smith, 2017).

Tectonite (unit 9)

Tectonite of unit 9 comprises mafic to felsic mylonite to protomylonite within the JSZ (Figure GS2019-2-2), characterized by the development of intense S_2 tectonic fabrics. The protoliths of such high-strain rocks are difficult to determine in the field, although some feldspar and quartz relicts may be partly preserved in felsic tectonite that shows brittle-ductile deformation (Figure GS2019-2-8c, d). Mafic tectonites derived from mafic volcanic flows and/or volcaniclastic rocks are indistinguishable, particularly those that were altered to very fine grained chlorite and sericite. Quartz veins or veinlets in tectonite are concentrated primarily along the S_2 foliation. Asymmetric quartz boudins are a reliable shear-sense indicator (e.g., dextral shear, as shown in Figure GS2019-2-8e).

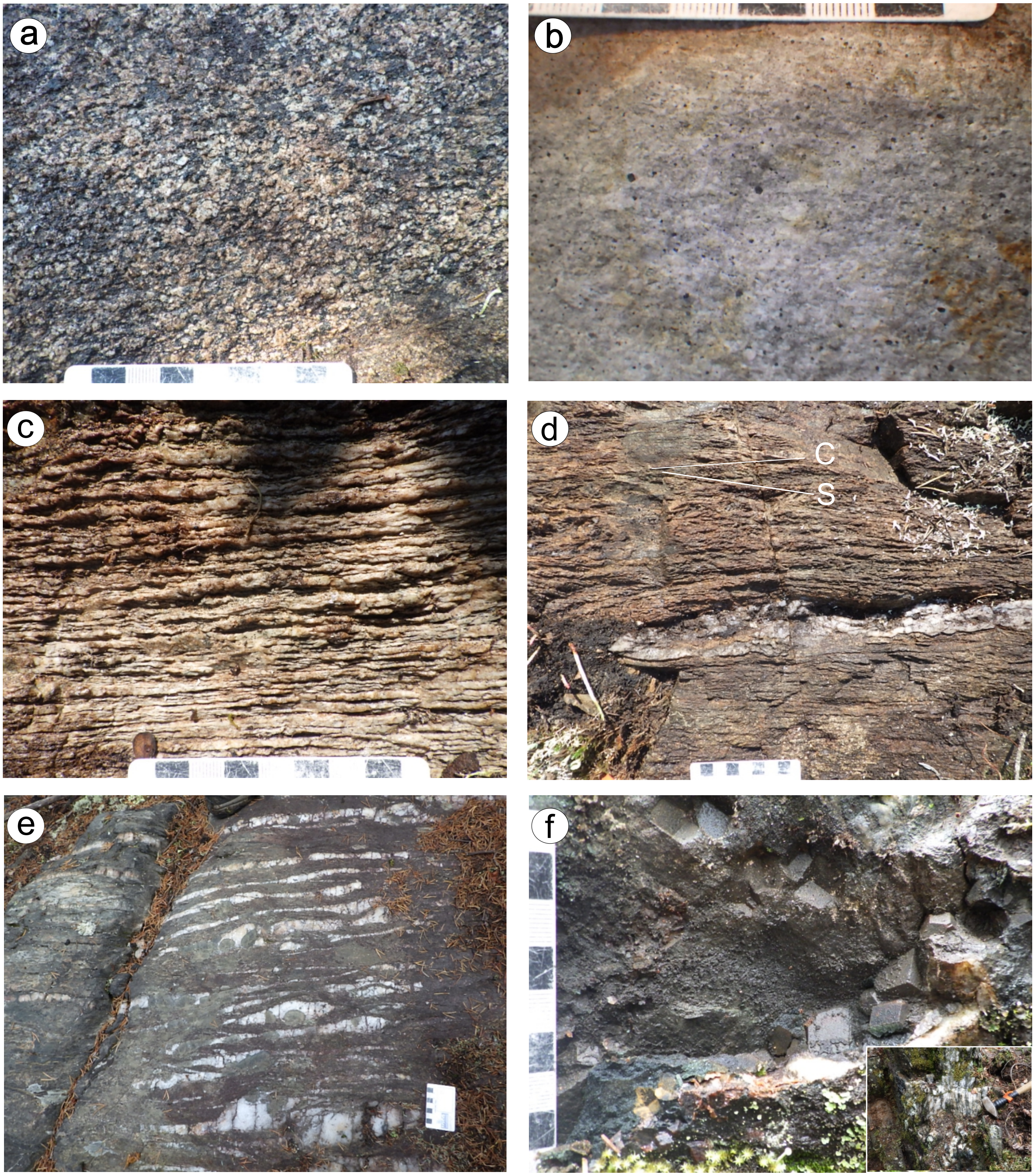

Figure GS2019-2-8: *Outcrop photographs of units 7, 8 and 9 in the Gemmell Lake area:* ***a)*** *weakly foliated, massive, coarse-grained quartz diorite (subunit 7a; UTM Zone 14N, 365243E, 6292252N, NAD 83);* ***b)*** *massive quartz-feldspar porphyry with up to 2% euhedral to subhedral magnetite (up to 3 mm) phenocrysts (unit 8; UTM 363619E; 6283902N);* ***c)*** *dacitic to rhyolitic mylonite showing brittle-ductile fabrics (S_2) and shear bands (unit 9; UTM 367059E, 6290899N);* ***d)*** *S-C fabric indicative of sinistral shear in felsic protomylonite with boudinaged quartz in dominant S_2 plane that cuts shallowly dipping S_1 fabrics (unit 9; UTM 367020E, 6290960N);* ***e)*** *silicified mafic mylonite cut by numerous quartz veins along a subvertical shear zone; dextral shear sense indicated by the asymmetric sigmoid quartz at the bottom of the photo (unit 9; UTM 359555E, 6288809N);* ***f)*** *quartz vein (~30 cm in width as shown by inset photo in lower right corner) containing megacrystic euhedral garnet crystals, which was emplaced along the contact between sheared unit 1 dacitic to rhyolitic rock and unit 2 basalt (UTM 362308E, 6289245N).*

Within the JSZ, an approximately 30 cm wide quartz vein occurs along the contact between strongly sheared felsic and mafic rocks south of Gemmell Lake. This quartz vein contains maroon, megacrystic, euhedral garnet crystals (up to 1.5 cm; Figure GS2019-2-8f) together with acicular amphibole and chlorite concentrated toward the mafic side, whereas smaller (3–5 mm) garnet crystals cluster in the central part of the vein.

Structural geology

Six regional deformation events (D_1 to D_6) were defined in the LLGB (Beaumont-Smith and Böhm, 2002, 2004). Structures related to D_1 deformation are represented by penetrative, shallow-dipping S_1 foliation (e.g., Figure GS2019-2-8c) overprinted by vertical S_2 fabrics associated with D_2 deformation. Although locally preserved in the Wasekwan group supracrustal rocks, D_1 fabrics are not evident in the Sickle group, Pool lake suite (Gilbert et al., 1980; Anderson and Beaumont-Smith, 2001) or pre-Sickle intrusive suite rocks (this study). Therefore, D_1 deformation likely reflects the assembly of volcanic terranes that constitute the LLGB (e.g., Beaumont-Smith and Böhm, 2002, 2004).

In the Gemmell Lake area, D_2 structures are the most penetrative and manifest as a steeply north-dipping S_2 foliation and tight to isoclinal folds (F_2) that have shallowly plunging hinges and associated minor chevron folds. Foliations of this deformation (S_2) were observed in all map units except the late intrusive suite. Typically, S_2 foliations dip steeply to the north and contain a down-dip to steeply plunging mineral and stretching lineation (e.g., Sherman, 1992; Anderson and Beaumont-Smith, 2000; Beaumont-Smith et al., 2001). These L_2 lineations are well defined by a preferred orientation of minerals (e.g., amphibole, biotite, feldspar), stretched pillows and flattened pebbles and cobbles (e.g., Figure GS2019-2-7d).

Ductile shear zones that generally define map-unit contacts are commonly related to D_2 deformation, as the intensity of S_2 fabrics and tightness of F_2 folds increase toward contacts. The D_2 shear zones are characterized by dextral shear-sense indicators (e.g., Figure GS2019-2-7e) on horizontal surfaces and steeply plunging, generally down-dip to slightly oblique (easterly pitch) stretching lineations.

The Johnson shear zone (JSZ), a regional east-trending shear zone, transects the southern part of the map area (Figure GS2019-2-1) and can be traced more than 100 km along strike. The JSZ is a dominantly dextral transpressional fault zone (Beaumont-Smith and Rogge, 1999; Jones, 2005; Jones et al., 2006). Numerous dextral shear-sense indicators (e.g., shear bands, S-C fabrics, asymmetric quartz boundins, rotated garnet porphyroblasts) were observed on the horizontal surface within the JSZ. The development of narrow zones of shallowly plunging stretching lineations in the core of the shear zone reflects kinematics consistent with shear-zone development in response to dextral transpression. Similar shear zones (e.g., the North Stear Lake shear zone and Pool Lake fault zone; Beaumont-Smith, 2001; this study) are parallel to subparallel to the JSZ and could also be associated with D_2 deformation (Figure GS2019-2-2).

The D_3 deformation is represented in the map area by close to tight, S-asymmetric F_3 folds and northwest-trending, axial-planar S_3 crenulation cleavage. A set of northwest- to west-northwest-trending faults (e.g., the Boiley Lake shear zone; Figure GS2019-2-2) is thought to be related to the D_3 event. F_4 folds are also pervasive throughout the map area. These folds plunge steeply to the northeast and are associated with steeply dipping, northeast-striking, axial-planar S_4 crenulation cleavage. The Gemmell Lake fault and Motriuk Lake–Jones Lake fault strike north-northeast and display sinistral movement, which is likely associated with D_4 deformation. Mesoscopic structures associated with D_5 deformation include open F_5 conjugate folds, kink bands and crenulations, and a brittle D_5 fault.

The D_6 deformation was brittle to ductile and represented by sinistral reactivation of D_2 shear zones (Figure GS2019-2-8d; Beaumont-Smith and Böhm, 2004). In places, retrograde actinolite crystals (up to 1.5 cm in length) are randomly oriented on the planes of associated planar structures (cleavages, fractures). The garnet-bearing quartz veins shown in Figure GS2019-2-8f may have formed at this stage.

Economic considerations

New mapping of the LLGB in the Gemmell Lake area suggests that rheological differences between volcaniclastic rocks (unit 1), Fe-rich mafic volcanic rocks (unit 2) and sedimentary rocks (unit 3) acted as foci for ductile strain during multiple phases of deformation along the JSZ and associated subsidiary D_2 structures, focusing Au-bearing fluids into structural and chemical traps. Potential structural traps include areas where D_2 shear zones and D_3 and D_4 structures intersect, as these may form dilatant zones.

To the east of the Motriuk Lake–Jones Lake fault, the McBride Au occurrence (Figure GS2019-2-2) consists of north-northeast-trending Au-bearing quartz-vein systems cutting an unexposed quartz diorite intrusion emplaced within the JSZ (Ferreira, 1993). Historical drill data indicate that significant intersections returned 373.5 g/t Au over

0.4 m and 7.9 g/t over 2.5 m (Assessment File 72937). The McBride quartz diorite could be part of the Motriuk Lake pluton (subunit 7a; Yang and Beaumont-Smith, 2015c) about 1.2 km to the north. The latter body displays a geochemical signature similar to that of the quartz diorite intrusion at the southern margin of the Gordon Au deposit in the Farley Lake area of the northern belt (Yang and Beaumont-Smith, 2016). Notably, the Farley Lake quartz diorite has an adakite-like signature and has been attributed to the post-Sickle intrusive suite (Yang and Lawley, 2018).

Recent studies suggest that rollback of a subducting slab may have resulted in upwelling of asthenosphere and partial melting of previously metasomatized lithospheric mantle. The resulting adakitic melts could transfer Au and other metals from the mantle (Holwell et al, 2019) or lower crust (Hou and Wang, 2019) to the middle to upper crust along deep fault systems (e.g., the JSZ), forming Au deposits aided by favourable chemical-structural traps. Therefore, occurrences of adakite-like intrusions as part of the post-Sickle intrusive suite in the LLGB are worthy of further study in terms of mineral targeting.

The Finlay McKinlay Au occurrence (Ferreira, 1993) also comprises Au-bearing quartz veins in an approximately 10 m wide north-northeast-trending shear zone that can be traced about 100 m along strike and cuts a quartz diorite intrusion (subunit 7a). Bulk-rock sampling from the quartz veins yielded 17 g/t Au (Sherman et al., 1989), not only confirming the presence of visible Au (Baldwin, 1987) but also highlighting the importance of granitoid-hosted Au-bearing quartz-vein systems. More importantly, the association of Te minerals (e.g., hessite [Ag_2Te], tellurobismuthite [Bi_2Te_3]; see Sherman, 1992) within the Au-bearing quartz-vein systems suggests that auriferous fluids may have been sourced from granitoid magmas derived from the mantle (e.g., Holwell et al., 2019) to the lower crust (Hou and Wang, 2019). The quartz diorite intrusion displaying a relative magnetic low is in structural contact with Sickle group polymictic conglomerate (subunit 6b) that appears to have been thrust over the intrusion.

The Gemmell Lake Au occurrence is hosted in mylonite and silicified-sericitized rhyolitic to dacitic volcanic to volcaniclastic rocks (subunit 1a and unit 9) within the JSZ and related structures in the west Gemmell Lake area (Beaumont-Smith and Edwards, 2000). Unlike most Au deposits of the LLGB, the Gemmell Lake occurrence lacks a relatively reducing chemical trap (e.g., Fe-rich mafic volcanic to volcaniclastic rocks at MacLellan and Burnt Timber, BIFs at Gordon). However, the intersection of silicification and sulphidization (disseminated arsenopyrite, pyrite) of mylonitized felsic volcanic to volcaniclastic rocks controlled by D_2 deformation with D_3 faults may have created favourable structural site(s) for Au precipitation.

South of Boiley Lake, VMS Cu-(Au-Zn) mineralization is hosted in subunit 1c garnet-biotite schist that constitutes the major portion of the Boiley Lake alteration zone (Gale, 1983; Ferreira, 1993; Anderson and Beaumont-Smith, 2001). Drillhole intersections returned 2.02% Cu and 1.2 g/t Au over 0.8 m (Assessment File 92793). The area contains both muscovite-bearing granite (pre-Sickle intrusive suite; subunit 5c) and magnetite-phyric quartz-feldspar porphyry (late intrusive suite; unit 8). The sources of auriferous fluids are the subject of ongoing collaborative research between the Manitoba Geological Survey and the Geological Survey of Canada (GSC). It is worth noting that the fluid sources may be tracked by investigation of the partitioning behaviour of rare-earth elements in magmatic-hydrothermal systems (e.g., Yang, 2019b).

Acknowledgments

The author thanks M. Kohli for providing enthusiastic field assistance; E. Anderson for thorough logistical support; L. Chackowsky for technical support; and C. Epp for cataloguing, processing and preparing the samples. C.J.M. Lawley of the GSC is thanked for communication of detrital U-Pb zircon age data. Thanks go to Alamos Gold Inc. for generously providing detailed airborne geophysical data. The manuscript benefited greatly from constructive reviews by M. Rinne, K.D. Reid and C.O. Böhm, and from technical editing by R.F. Davie.

References

Anderson, S.D. and Beaumont-Smith, C.J. 2001: Structural analysis of the Pool Lake–Boiley Lake area, Lynn Lake greenstone belt (NTS 64C/11); *in* Report of Activities 2001, Manitoba Industry, Trade and Mines, Manitoba Geological Survey, p. 76–85.

Ansdell, K.M. 2005: Tectonic evolution of the Manitoba-Saskatchewan segment of the Paleoproterozoic Trans-Hudson Orogen, Canada; Canadian Journal of Earth Sciences, v. 42, p. 741–759.

Ansdell, K.M., Corrigan, D., Stern, R. and Maxeiner, R. 1999: SHRIMP U-Pb geochronology of complex zircons from Reindeer Lake, Saskatchewan: implications for timing of sedimentation and metamorphism in the northwestern Trans-Hudson Orogen; Geological Association of Canada–Mineralogical Association of Canada, Joint Annual Meeting, Program with Abstracts, v. 24, p. 3.

Baldwin, D.A. 1987: Gold mineralization associated with the Johnson Shear Zone; *in* Report of Field Activities 1987, Manitoba Energy and Mines, Minerals Division, p. 7–11.

Baldwin, D.A., Syme, E.C., Zwanzig, H.V., Gordon, T.M., Hunt, P.A. and Stevens, R.P. 1987: U-Pb zircon ages from the Lynn Lake and Rusty Lake metavolcanic belts, Manitoba: two ages of Proterozoic magmatism; Canadian Journal of Earth Sciences, v. 24, p. 1053–1063.

Baragar, W.R.A., Ernst, R.E., Hulbert, L. and Peterson, T. 1996: Longitudinal petrochemical variation in the Mackenzie dyke swarm, northwestern Canadian Shield; Journal of Petrology, v. 37, p. 317–359.

Bateman, J.D. 1945: McVeigh Lake area, Manitoba; Geological Survey of Canada, Paper 45-14, 34 p.

Beaumont-Smith, C.J. 2008: Geochemistry data for the Lynn Lake greenstone belt, Manitoba (NTS 64C11-16); Manitoba Science, Technology, Energy and Mines, Manitoba Geological Survey, Open File OF2007-1, 5 p.

Beaumont-Smith, C.J. and Böhm, C.O. 2002: Structural analysis and geochronological studies in the Lynn Lake greenstone belt and its gold-bearing shear zones (NTS 64C10, 11, 12, 14, 15 and 16), Manitoba; *in* Report of Activities 2002, Manitoba Industry, Trade and Mines, Manitoba Geological Survey, p. 159–170.

Beaumont-Smith, C.J. and Böhm, C.O. 2003: Tectonic evolution and gold metallogeny of the Lynn Lake greenstone belt, Manitoba (NTS 64C10, 11, 12, 14, 15 and 16), Manitoba; *in* Report of Activities 2003, Manitoba Industry, Economic Development and Mines, Manitoba Geological Survey, p. 39–49.

Beaumont-Smith, C.J. and Böhm, C.O. 2004: Structural analysis of the Lynn Lake greenstone belt, Manitoba (NTS 64C10, 11, 12, 14, 15 and 16); *in* Report of Activities 2004, Manitoba Industry, Economic Development and Mines, Manitoba Geological Survey, p. 55–68.

Beaumont-Smith, C.J. and Edwards, C.D. 2000: Detailed structural analysis of the Johnson Shear Zone in the west Gemmell Lake area (NTS 64C/11); *in* Report of Activities 2000, Manitoba Industry, Trade and Mines, Manitoba Geological Survey, p. 64–68.

Beaumont-Smith, C.J. and Rogge, D.M. 1999: Preliminary structural analysis and gold metallogeny of the Johnson Shear Zone, Lynn Lake greenstone belt (parts of NTS 64C/10, 11, 15); *in* Report of Activities 1999, Manitoba Industry, Trade and Mines, Geological Services, p. 61–66.

Beaumont-Smith, C.J., Anderson, S.D. and Böhm, C.O. 2001: Structural analysis and investigations of shear-hosted gold mineralization in the southern Lynn Lake greenstone belt (parts of NTS 64C/11, /12, /15, /16); *in* Report of Activities 2001, Manitoba Industry, Trade and Mines, Manitoba Geological Survey, p. 67–75.

Beaumont-Smith, C.J., Machado, N. and Peck, D.C. 2006: New uranium-lead geochronology results from the Lynn Lake greenstone belt, Manitoba (NTS 64C11-16); Manitoba Science, Technology, Energy and Mines, Manitoba Geological Survey, Geoscientific Paper GP2006-1, 11 p.

Boyle, R.W. 1979: The geochemistry of gold and its deposits (together with a chapter on geochemical prospecting for the element); Geological Survey of Canada, Bulletin 280, 584 p.

Corrigan, D. 2012: Paleoproterozoic crustal evolution and tectonic processes: insights from the Lithoprobe program in the Trans-Hudson orogen, Canada; Chapter 4 *in* Tectonic Styles in Canada: The LITHOPROBE Perspective, J.A. Percival, F.A. Cook and R.M. Clowes (ed.), Geological Association of Canada, Special Paper 49, p. 237–284.

Corrigan, D., Galley, A.G. and Pehrsson, S. 2007: Tectonic evolution and metallogeny of the southwestern Trans-Hudson Orogen; *in* Mineral Deposits of Canada: A Synthesis of Major Deposit-Types, District Metallogeny, the Evolution of Geological Provinces, and Exploration Methods, W.D. Goodfellow (ed.), Geological Association of Canada, Mineral Deposits Division, Special Publication 5, p. 881–902.

Corrigan, D., Pehrsson, S., Wodicka, N. and de Kemp, E. 2009: The Palaeoproterozoic Trans-Hudson Orogen: a prototype of modern accretionary processes; *in* Ancient Orogens and Modern Analogues, J.B. Murphy, J.D. Keppie, and A.J. Hynes (ed.), Geological Society of London, Special Publications, v. 327, p. 457–479.

Fedikow, M.A.F. 1986: Geology of the Agassiz stratabound Au-Ag deposit, Lynn Lake, Manitoba; Manitoba Energy and Mines, Geological Services, Open File Report OF85-5, 80 p.

Fedikow, M.A.F. 1992: Rock geochemical alteration studies at the MacLellan Au-Ag deposit, Lynn Lake, Manitoba; Manitoba Energy and Mines, Geological Services, Economic Geology Report ER92-1, 237 p.

Fedikow, M.A.F. and Gale, G.H. 1982: Mineral deposit studies in the Lynn Lake area; *in* Report of Field Activities 1982, Manitoba Department of Energy and Mines, Mineral Resources Division, p. 44–54.

Fedikow, M.A.F. Ferreira, K.J. and Baldwin, D.A. 1991: The Johnson shear zone – a regional metallogenetic feature in the Lynn Lake area; Manitoba Energy and Mines, Geological Services, Minerals Division, Mineral Deposit Thematic Map MDT91-1, scale 1:50 000.

Ferreira, K.J. 1993: Mineral deposits and occurrences in the McGavock Lake area, NTS 64C/11; Manitoba Energy and Mines, Geological Services, Mineral Deposit Series Report No. 26, 49 p.

Gale, G.H. 1983: Mineral deposit investigations in the Lynn Lake area; *in* Report of Field Activities 1983, Manitoba Department of Energy and Mines, Mineral Resources Division, p. 84–87.

Gilbert, H.P. 1993: Geology of the Barrington Lake–Melvin Lake–Fraser Lake area; Manitoba Energy and Mines, Geological Services, Geological Report GR87-3, 97 p.

Gilbert, H.P., Syme, E.C. and Zwanzig, H.V. 1980: Geology of the metavolcanic and volcaniclastic metasedimentary rocks in the Lynn Lake area; Manitoba Energy and Mines, Mineral Resources Division, Geological Paper GP80-1, 118 p.

Glendenning, M.W.P., Gagnon, J.E. and Polat, A. 2015: Geochemistry of the metavolcanic rocks in the vicinity of the MacLellan Au-Ag deposit and an evaluation of the tectonic setting of the Lynn Lake greenstone belt, Canada: evidence for a Paleoproterozoic-aged rifted continental margin; Lithos, v. 233, p. 46–68.

Hastie, E.C.G., Gagnon, J.E. and Samson, I.M. 2018: The Paleoproterozoic MacLellan deposit and related Au-Ag occurrences, Lynn Lake greenstone belt, Manitoba: an emerging, structurally controlled gold camp; Ore Geology Reviews, v. 94, p. 24–45.

Hoffman, P.H. 1988: United plates of America, the birth of a craton: Early Proterozoic assembly and growth of Laurentia; Annual Reviews of Earth and Planetary Sciences, v. 16, p. 543–603.

Holwell, D.A., Fiorentini, M., McDonald, I., Lu, Y., Giuliani, A., Smith, D.J., Keith, M. and Locmelis, M. 2019: A metasomatized lithospheric mantle control on the metallogenic signature of post-subduction magmatism; Nature Communication, v. 10, p. 3511, URL <https://doi.org/10.1038/s41467-019-11065-4> [October 2019].

Hou, Z. and Wang, R. 2019: Fingerprinting metal transfer from mantle; Nature Communication, v. 10, p. 3510, URL <https://doi.org/10.1038/s41467-019-11445-w> [October 2019].

Jones, L.R. 2005: Geology of the shear-hosted Burnt Timber deposit, Lynn, northern Manitoba; M.Sc. thesis, Laurentian University, Sudbury, Ontario, 63 p.

Jones, L.R., Lafrance, B. and Beaumont-Smith, C.J. 2006: Structural controls on gold mineralization at the Burnt Timber Mine, Lynn Lake Greenstone Belt, Trans-Hudson Orogen, Manitoba; Exploration and Mining Geology, v. 15, p. 89–100.

Kremer, P.D., Rayner, N. and Corkery, M.T. 2009: New results from geological mapping in the west-central and northeastern portions of Southern Indian Lake, Manitoba (parts of NTS 64G1, 2, 8, 64H4, 5); *in* Report of Activities 2009, Manitoba Science, Innovation, Energy and Mines, Manitoba Geological Survey, p. 94–107.

Lawley, C.J.M, Davis, W.J., Jackson, S.E., Petts, D.C., Yang, E., Zhang, S. Selby, D., O'Connor, A.R. and Schneider, D.A. 2019: Paleoproterozoic gold and its tectonic triggers and traps; *in* Targeted Geoscience Initiative: 2018 report of activities, N. Rogers (ed.), Geological Survey of Canada, Open File 8549, p. 71–75.

Lewry, J.F. and Collerson, K.D. 1990: The Trans-Hudson Orogen: extent, subdivisions and problems; *in* The Early Proterozoic Trans-Hudson Orogen of North America, J.F. Lewry and M.R. Stauffer (ed.), Geological Association of Canada, Special Paper 37, p. 1–14.

Ma, G. and Beaumont-Smith, C.J. 2001: Stratigraphic and structural mapping of the Agassiz Metallotect near Lynn Lake, Lynn Lake greenstone belt (parts of NTS 64C/14, /15); *in* Report of Activities 2001, Manitoba Industry, Trade and Mines, Manitoba Geological Survey, p. 86–93.

Ma, G., Beaumont-Smith, C.J. and Lentz, D.R. 2000: Preliminary structural analysis of the Agassiz Metallotect near the MacLellan and Dot lake gold deposits, Lynn Lake greenstone belt (parts of NTS 64C/14, /15); *in* Report of Activities 2000, Manitoba Industry, Trade and Mines, Manitoba Geological Survey, p. 51–56.

Manitoba Energy and Mines 1986: Granville Lake, NTS 64C; Manitoba Energy and Mines, Minerals Division, Bedrock Geology Compilation Map Series, Map 64C, scale 1:250 000.

Martins, T., Kremer, P.D., Corrigan, D. and Rayner, N. 2019: Geology of the Southern Indian Lake area, north-central Manitoba (parts of NTS 64G1, 2, 7–10, 64H3–6); Manitoba Growth, Enterprise and Trade, Manitoba Geological Survey, Geoscientific Report GR2019-1, 51 p. and 4 colour maps at 1:50 000 scale.

Milligan, G.C. 1960: Geology of the Lynn Lake district; Manitoba Department of Mines and Natural Resources, Mines Branch, Publication 57-1, 317 p.

Norman, G.W.H. 1933: Granville Lake district, northern Manitoba; Geological Survey of Canada, Summary Report, Part C, p. 23–41.

Park, A.F., Beaumont-Smith, C.J. and Lentz, D.R. 2002: Structure and stratigraphy in the Agassiz Metallotect, Lynn Lake greenstone belt (NTS 64C/14 and /15), Manitoba; *in* Report of Activities 2002, Manitoba Industry, Trade and Mines, Manitoba Geological Survey, p. 171–186.

Peck, D.C., Lin, S., Atkin, K. and Eastwood, A.M. 1998: Reconnaissance structural studies of Au metallotects in the Lynn Lake greenstone belt (parts of NTS 63C/10, C/11, C/15); *in* Report of Activities 1998, Manitoba Energy and Mines, Geological Services, p. 69–74.

Sherman, G.R. 1992: Geology, hydrothermal activity and gold mineralization in the Gemmell Lake area of the early Proterozoic Lynn Lake greenstone belt, Manitoba; M.Sc. thesis, University of Windsor, Windsor, Ontario, 148 p.

Sherman, G.R., Samson, I.M. and Holm, P.E. 1988: Preliminary observations of a detailed geological investigation of the Gemmell Lake area, Lynn Lake; *in* Report of Field Activities 1988, Manitoba Energy and Mines, Minerals Division, p. 16–19.

Sherman, G.R. Samson, I.M. and Holm, P.E. 1989: Deformation, veining and gold mineralization along part of the Johnson shear zone, Lynn Lake greenstone belt, Manitoba; *in* Report of Field Activities 1989; Manitoba Energy and Mines; Minerals Division, p. 16–18.

Stauffer, M.R. 1984: Manikewan: an Early Proterozoic ocean in central Canada, its igneous history and orogenic closure; Precambrian Research, v. 25, p. 257–281.

Stern, R.A., Syme, E.C. and Lucas, S.B. 1995: Geochemistry of 1.9 Ga MORB- and OIB-like basalts from the Amisk collage, Flin Flon Belt, Canada: evidence for an intra-oceanic origin; Geochimica et Cosmochimica Acta, v. 59, p. 3131–3154.

Syme, E.C. 1985: Geochemistry of metavolcanic rocks in the Lynn Lake Belt; Manitoba Energy and Mines, Geological Services/Mines Branch, Geological Report GR84-1, 84 p.

Turek, A., Woodhead, J. and Zwanzig H.V. 2000: U-Pb age of the gabbro and other plutons at Lynn Lake (part of NTS 64C); *in* Report of Activities 2000, Manitoba Industry, Trade and Mines, Manitoba Geological Survey, p. 97–104.

Yang, X.M. 2019a: Bedrock geology of the Gemmell Lake area, Lynn Lake greenstone belt, northwestern Manitoba (parts of NTS 64C11, 14); Manitoba Agriculture and Resource Development, Manitoba Geological Survey, Preliminary Map PMAP2019-2, scale 1:20 000.

Yang, X.M. 2019b: Using rare earth elements (REE) to decipher the origin of ore fluids associated with granite intrusions; Minerals, v. 9, p. 426, URL <https://doi.org/10.3390/min9070426> [October 2019].

Yang, X.M. and Beaumont-Smith, C.J. 2015a: Bedrock geology of the Keewatin River area, Lynn Lake greenstone belt, northwestern Manitoba (parts of NTS 64C14, 5); Manitoba Mineral Resources, Manitoba Geological Survey, Preliminary Map PMAP2015-3, scale 1:20 000.

Yang, X.M. and Beaumont-Smith, C.J. 2015b: Geological investigations of the Keewatin River area, Lynn Lake greenstone belt, northwestern Manitoba (parts of NTS 64C14, 15); *in* Report of Activities 2015, Manitoba Mineral Resources, Manitoba Geological Survey, p. 52–67.

Yang, X.M. and Beaumont-Smith, C.J. 2015c: Granitoid rocks in the Lynn Lake region, northwestern Manitoba: preliminary results of reconnaissance mapping and sampling; *in* Report of Activities 2015, Manitoba Mineral Resources, Manitoba Geological Survey, p. 68–78.

Yang, X.M. and Beaumont-Smith, C.J. 2016: Geological investigations in the Farley Lake area, Lynn Lake greenstone belt, northwestern Manitoba (part of NTS 64C16); *in* Report of Activities 2016, Manitoba Growth, Enterprise and Trade, Manitoba Geological Survey, p. 99–114.

Yang, X.M. and Beaumont-Smith, C.J. 2017: Bedrock geology of the Wasekwan Lake area, Lynn Lake greenstone belt, northwestern Manitoba (parts of NTS 64C10, 15); Manitoba Growth, Enterprise and Trade, Manitoba Geological Survey, Preliminary Map PMAP2017-3, scale 1:20 000.

Yang, X.M. and Lawley, C.J.M. 2018: Tectonic setting of the Gordon gold deposit, Lynn Lake greenstone belt, northwestern Manitoba (parts of NTS 64C16): evidence from lithogeochemistry, Nd isotopes and U-Pb geochronology; *in* Report of Activities 2018, Manitoba Growth, Enterprise and Trade, Manitoba Geological Survey, p. 89–109.

Zwanzig, H.V. and Bailes, A.H. 2010: Geology and geochemical evolution of the northern Flin Flon and southern Kisseynew domains, Kississing–File lakes area, Manitoba (parts of NTS 63K, N); Manitoba Innovation, Energy and Mines, Manitoba Geological Survey, Geoscientific Report GR2010-1, 135 p.

Zwanzig, H.V., Syme, E.C. and Gilbert, H.P. 1999: Updated trace element geochemistry of ca. 1.9 Ga metavolcanic rocks in the Paleoproterozoic Lynn Lake belt; Manitoba Industry, Trade and Mines, Geological Services, Open File Report OF99-13, 46 p.